

Suppression of core polarization in halo nuclei

T.T.S. Kuo¹, F. Krmpotić², and Y. Tzeng³

¹*Department of Physics, SUNY-Stony Brook*

Stony Brook, New York 11794 USA

² *Departamento de Física, Facultad de Ciencias Exactas*

Universidad Nacional de La Plata, C. C. 67, 1900 La Plata, Argentina

³ *Institute of Physics, Academia Sinica*

Nankang, Taipei, Taiwan

(December 2, 2024)

Abstract

The effect of core polarization in halo nuclei is studied using a two -frequency shell-model approach: $\hbar\omega_{in}$ for the inner orbits and $\hbar\omega_{out}$ for the outer (halo) orbits. Starting from the Paris and Bonn NN potentials, accurate model-space G -matrix is first derived. The core-polarization diagrams G_{3p1h} are then evaluated as a function of $\hbar\omega_{out}$, with $\hbar\omega_{in}$ held fixed. We find that they are largely suppressed for halo nuclei such as 6He , 6Li and ^{11}Li . The calculated *di-neutron* $(p_{3/2})^2$ and $(p_{1/2})^2$ and *proton-neutron* $(p_{3/2})^2$ energies in these nuclei are also in good agreement with experiments. It is suggested that the fundamental NN interaction can be probed in a clearer and more direct way in halo nuclei than in ordinary nuclei.

PACS numbers: 21.30.+y, 21.60.Cs, 21.90.+f

Radioactive-beam nuclear physics has been progressing rapidly, and there is much current interest in studying halo nuclei. [1] In a recent issue of Physical Review C, there were four articles about halo nuclei: Nazarewicz *et al.*, [2] dealt with the halo nuclei around the nucleus ^{48}Ni , which is a mirror image of ^{48}Ca that is a "best" closed-shell nucleus. It is remarkable that nuclei as exotic as ^{48}Ni are now being studied! In the drip-line nuclei, Hamamoto *et al.*, [3] have carried out a systematic investigation of the single particle and collective degrees of freedom, both of them playing a central role in building up the structure of halo nuclei. There is also an experimental study of heavy halo nuclei around $N = 82$ [4].

Halo nuclei, or drip-line nuclei are generally barely bound (or unbound) and their structure is typically that of a tightly bound inner core with a few outer nucleons that are loosely attached to the core. For example, the halo nucleus 6He is presumably made of a 4He core with a pair of loosely-attached outer nucleons. The outer nucleons are spatially extended and have a large rms radius R . In fact, $R^{exp}(^6He) \cong 2.6$ fm [5] corresponds to a $\hbar\omega$ value considerably smaller than that given by the empirical formula $\hbar\omega = 45A^{-1/3} - 25A^{-2/3}$ (valid for ordinary stable nuclei).

Although the halo nucleons are distantly separated from each other and from the core, the interaction among themselves plays a delicate role in halo nuclei. For instance, while 6He as a whole is bound its binary subsystems, *i.e.*, 5He and the "di-neutron" are unbound. Therefore the di-neutron interaction energy, though small, is crucial for the binding of 6He , and it is important to calculate it as accurately as we can.

So far, halo nuclei have been calculated using empirical effective interactions such as the Skyrme forces [2,3]. This clearly can be improved upon. Empirical effective interactions have been designed to fit the properties of ordinary nuclei, in the stable nuclear region. It is uncertain whether their application can be extended to exotic nuclei like the halo nuclei. Halo nucleons are usually far and away from the nuclear core and in a sparsely populated region; the interaction among them should predominately be the free nucleon-nucleon (NN) interaction such as the Paris [6] and Bonn [7] interactions, with little medium corrections due to the presence of other nucleons in the nucleus. It is thus useful and of interest to carry

out a derivation of the effective interaction (V_{eff}) for halo nucleons starting from a basic NN interaction.

In this letter, we wish to report a microscopic derivation of V_{eff} for halo nucleons, using a G -matrix folded-diagram approach [8,9]. The Paris and Bonn NN potentials will be employed. In addition, we would like to advocate that V_{eff} among the halo nucleons, such as those in the di-neutron mentioned earlier, can be more reliably calculated, from first principles, than that for nucleons in ordinary nuclei. A major difficulty in microscopic effective interaction theories has been the treatment of the core polarization effect (CPE), in particular the higher-order core polarization diagrams. As we shall discuss later, the physical environment in halo nuclei provides a natural suppression of the CPE. And V_{eff} should be given largely by the G -matrix alone, which presently can be calculated to a high degree of accuracy. Thus it is likely that halo nuclei, besides having excitingly interesting and exotic properties, also may provide a much better testing ground for the fundamental NN interactions, than ordinary nuclei.

Starting from a free NN interaction, the model-space V_{eff} can be derived microscopically using a G -matrix folded-diagram approach [8,9]. The main steps in such a derivation are: choice of the model space P , calculation of the model-space G -matrix, and calculation of the irreducible diagrams for the vertex function \hat{Q} -boxes. Let us now discuss the application of the above framework to halo nuclei.

An important criterion for choosing a model space P is that the P -space overlaps of the physical states under consideration should be as large as possible. Consider 6He as an example. Its core is 4He , which should remain essentially as an ordinary alpha particle, with little perturbation from the distant halo nucleons. We shall use a model space of a closed $(0s_{1/2})^4$ core, the alpha particle, with the valence (halo) nucleons confined in the $0p$ shell. The core has a small rms radius while the halo nucleons have a much larger rms radius. It would not be feasible to reproduce both the small and large rms radii, using shell model wave functions of a common oscillator constant $\hbar\omega$. One may get past this difficulty by including several major shells in the one-frequency shell model (OFSM) calculation. But this would be

very tedious. A convenient and physically appealing solution to this problem is to employ a two-frequency shell model (TFSM) for the description of halo nuclei, as suggested by Kuo *et al.*, [10]. (A preliminary application of their approach to 6He and 6Li have been carried out by them.)

Within the TFSM one uses oscillator wave functions with $\hbar\omega_{in}$ for the core (inner) orbits and those with $\hbar\omega_{out}$ for the halo (outer) orbits. (The notations b_{in} and b_{out} also will be used from now on, with $b^2 \equiv \hbar/m\omega$.) We shall study halo nuclei 6He , 6Li and ${}^{11}Li$ using the above mentioned P -space, with b_{in} fixed at 1.45 fm while treating b_{out} as a variation parameter (or generator coordinate).

For ordinary nuclei, there are now methods [11,12] by which the G -matrix can be calculated very accurately [11,12]. Let us extend them to the G -matrix for halo nucleons in the context of the above two-frequency model space. For a general model-space P , we define the corresponding Brueckner G -matrix by the integral equation [12,13]

$$G(\omega) = V + VQ_2 \frac{1}{\omega - Q_2 T Q_2} Q_2 G(\omega),$$

where ω is an energy variable. Q_2 is a two-body Pauli exclusion operator, and its treatment is very important. T is the two-nucleon kinetic energy. Note that our G -matrix has orthogonalized plane-wave intermediate states. The exact solution of this G -matrix is $G = G_F + \Delta G$ [11,12], where G_F is the "free" G -matrix, and ΔG is the Pauli correction term

$$\Delta G(\omega) = -G_F(\omega) \frac{1}{e} P_2 \frac{1}{P_2 [\frac{1}{e} + \frac{1}{e} G_F(\omega) \frac{1}{e} P_2]} P_2 \frac{1}{e} G_F(\omega),$$

where $e \equiv \omega - T$. The projection operator P_2 , defined as $(1 - Q_2)$, will be discussed later.

The basic ingredient for calculating the above G -matrix is the matrix elements of G_F , the free G -matrix, within the P_2 space. This space contains all the two-particle states that must be excluded from the intermediate states in G -matrix calculations. For ordinary nuclei, where the OFSM is used, the states excluded by the Pauli operator and those contained within the model space have a common length parameter b . For halo nuclei, where we use the TFSM, the situation is more complicated, as the excluded states and those within

the model space have in general wave functions of different length parameters, b_{in} and b_{out} . Hence to calculate ΔG , we need the matrix elements of G_F in a b_{in} - b_{out} mixed representation. This poses a technical difficulty because transformations for two-particle states with different oscillator lengths from the c.m. coordinates to the laboratory coordinates are not as easy to perform as for one common oscillator length. We have adopted an expansion procedure to surmount this difficulty, namely we expand the oscillator wave functions with b_{in} in terms of those with b_{out} , or *vice versa*. When b_{in} and b_{out} are not too different from each other, this procedure is relatively easy to carry out. Usually a high accuracy can be attained by including about 8 terms in the expansion. Still, the calculation of the two-frequency G -matrix is significantly more complicated than the ordinary one-frequency one.

Another difficulty about the derivation of the G -matrix for halo nuclei is the treatment of its Pauli exclusion operator. Halo nucleons are rather far from the other nucleons in the "core". This may mean that the effect of Pauli blocking is small, but it also suggests that to calculate a small effect reliably we need to do it with high accuracy.

We write the projection operator Q_2 as

$$Q_2 = \sum_{all \ ab} Q(ab)|ab\rangle\langle ab|,$$

where $Q(ab) = 0$, if $b \leq n_1, a \leq n_3$ or $b \leq n_2, a \leq n_2$ or $b \leq n_3, a \leq n_1$ and $Q(ab) = 1$ otherwise. The boundary of $Q(ab)$ is specified by the orbital numbers (n_1, n_2, n_3) . We denote the shell model orbits by numerals, starting from the bottom of the oscillator well, 1 for orbit $0s_{1/2}$, 2 for $0p_{3/2}, \dots, 7$ for $0f_{7/2}$ and so on. n_1 denotes the highest orbit of the closed core (Fermi sea). n_2 denotes the highest orbit of the chosen model space. We consider here 4He as a closed core, thus we have $n_1 = 1$. Suppose we use a model space including all the 6 orbits in the s, p and sd shells. Then for this case $n_2 = 6$. In principle one should take $n_3 = \infty$ [12], because we include only particle (above Fermi sea) states for the G -matrix intermediate states. In practice, this is not feasible, and one can only use a large n_3 determined by an empirical procedure. Namely, we perform calculations with increasing values for n_3 until numerical results become stable.

In Table 1, we display some representative results of our two-frequency G -matrix for the $\{0s0p\}$ model space, with $b_{in} = 1.45$ fm and $b_{out} = 2.0$ fm. We see that the difference between the free G -matrix (no Pauli blocking) and that with Pauli blocking is still significant, even though the halo nucleons are widely separated from the closed core. The only approximation here is the finite n_3 truncation. As seen from the table, a satisfactory n_3 convergence is attained when $n_3 = 21$, and the resulting G -matrix should be sufficiently accurate. This n_3 value will be used in the present work.

Using the above G -matrix, we can calculate the irreducible vertex function \hat{Q} -box, and then the model-space energy-independent V_{eff} is given by the \hat{Q} -box folded-diagram series [8,9]. A major uncertainty here has been to figure out what G -matrix diagrams should we, or can we, include in the \hat{Q} -box. The two leading terms are the well-known first-order G -matrix diagram and the second-order core polarization diagram G_{3p1h} [14]. Yet, there are many more higher-order core polarization diagrams. Hjorth-Jensen *et al.*, [15] have investigated the third-order \hat{Q} -box diagrams for the sd shell. After folding, the net effect on V_{eff} was a change of about $10 - 15\%$, as compared with the case when only the first- and second- order ones were considered. Higher and higher-order core polarization diagrams rapidly become prohibitively more difficult to deal with. Thus in practice one can only include some low-order diagrams for the calculation of the \hat{Q} -box.

The situation for the halo nucleons is different and may be promising. In ordinary nuclei, the valence nucleons are close to the nuclear core, an example being the two sd -shell neutrons of ^{18}O residing adjacently to the ^{16}O core. There is a strong valence-core coupling and hence a large CPE. The halo nucleons are located quite far away from the core. As we increase b_{out} , we are increasing the average distance between the halo nucleons and the core and so reducing the coupling between them. For sufficiently large b_{out} , the total CPE must be small and it should be sufficiently accurately given by the second-order (lowest order) core polarization diagram alone. This conjecture is supported by our results displayed in Fig. 1. We see that, as b_{out} increases, the core polarization diagrams G_{3p1h} approach rapidly and monotonically to zero. In fact they become negligibly small at $b_{out} \cong 2.25$ fm. This behavior

is understandable. As we illustrate in Fig. 2, the physical environment in ordinary nuclei is very different from that in halo nuclei. The halo nucleons are far and away from the core, and in this situation there is a natural suppression of the CPE.

The behavior of the bare G -interaction shown in Fig. 1 is also of interest. For the $p_{3/2}$ case, the interaction becomes weaker as b_{out} increases. Yet, this is not so for the $p_{1/2}$ case; here it becomes stronger as b_{out} increases. To assess this behaviour for the bare G -interaction, it may be useful to compare our results with experiments.

From mass tables [16], the valence interaction energy for 6He is

$$E_v^{exp}({}^6He) = -[\mathcal{B}({}^6He) + \mathcal{B}({}^4He) - 2\mathcal{B}({}^5He)] = -2.77 \text{ MeV}.$$

This energy is not yet comparable to the G -matrix that has an independent energy variable ω (see Eq.(1)), and we need to know what ω value one should use for G . (The G -matrix curves shown in Fig. 1 are for $\omega = -5$ MeV and Pauli exclusion operator with $(n_1, n_2, n_3) = (1, 3, 21)$). Furthermore, our model space has both $p_{3/2}$ and $p_{1/2}$ orbits. To calculate the above valence energy, we need to diagonalize a two-neutron ($T = 1, J = 0$) matrix in this space, using an energy-independent V_{eff} derived from the ω -dependent G -matrix. We have carried out such a derivation, following closely the \hat{Q} -box folded-diagram procedures of Ref. [14]. In this way we get $E_v^{th} = -2.77$ MeV at $b_{out} = 2.25$ fm for the Paris potential. As the CPE is strongly suppressed for such a b_{out} value, this result almost entirely comes from the bare G -matrix. The ground-state wave function of 6He is almost pure $(p_{3/2})^2$, with very little $(p_{1/2})^2$ admixture. Thus our E_v^{th} is also close to the diagonal G -matrix element shown in Fig. 1.

We have also calculated the valence interaction energy for 6Li using a similar folded-diagram procedure in the $p_{3/2} - p_{1/2}$ space. From the empirical masses of 6Li , 5Li , 5He and 4He [16], we obtain $E_v^{exp} = -3.88$ MeV. Our result is $E_v^{th} = -3.55$ MeV at $b_{out} = 2.25$ MeV for the Paris potential. Here the ($T = 0, J = 1$) ground-state wave function has a significant $(p_{1/2})^2$ component, as evidenced by the large difference between the diagonal $(p_{3/2})^2$ matrix element of Table 1 and E_v^{th} .

As we have used a $p_{3/2} - p_{1/2}$ model space, our wave function for ^{11}Li has only one component (neutron orbits closed). Then the diagonal $(p_{1/2})^2(T = 1, J = 0)$ matrix element of V_{eff} , which is quite close to the unfolded value of Fig.1 at $b_{out} = 2.25$ fm, is directly comparable to the valence interaction energy for ^{11}Li . From the masses of ^{11}Li , ^{10}Li and 9Li [16], we get $E_v^{exp} = -1.14$ MeV, while our result is $E_v^{th} = -0.79$ MeV at $b_{out} = -2.25$ fm for the Paris potential. This difference is an indication that the assumption of confining the valence ^{11}Li neutrons entirely to the p shell is not fully rightful. A larger space, such as $\{0p_{1/2}0d_{1s}\}$, is probable needed for them.

In passing, we mention that the above $b_{out} = 2.25$ fm is a reasonable choice. Recall that we have fixed $b_{in} = 1.45$ fm. With these values of b_{in} and b_{out} , and assuming a pure s^4p^n wave function, we get that $R^{th}(^6He) = 2.51$ fm, in good agreement with the empirical value $R^{exp}(^6He) = 2.57 \pm 0.1$ fm [5]; similarly, $R^{th}(^{11}Li) = 3.03$ fm while $R^{exp}(^{11}Li) = 3.1 \pm 0.1$ fm [5].

As a final comment, we point out that at large b_{out} the results given by the Paris and Bonn A potentials are practically identical with each other (see Fig. 1). This is because the halo nucleons are relatively distantly separated from each other, and the long-range parts of the different NN potential models do not differ much from each other.

In summary, we have attempted to derive the effective interaction for the valence nucleons in halo nuclei, starting from realistic NN interactions. Our preliminary results are encouraging. We have employed a two-frequency shell model approach, to give a good spatial description for both the core nucleons and the halo nucleons. While keeping the inner length parameter b_{in} fixed, we control the spatial extension of the halo nucleons by varying their length parameter b_{out} . In this way we have explicitly proved that the core polarization effect is strongly suppressed at large b_{out} values, as required by the large empirical rms radii of halo nuclei. This suggests that the effective interaction for halo nucleons is given predominantly by the bare G -matrix alone. For ordinary nuclei, when there are disagreements between theory and experiment, one is not sure if they are due to the NN interaction or to the approximation adopted in solving the many-body problems (such as the neglecting of

the higher-order core polarization diagrams). The situation for halo nuclei is much better, because of the inherent suppression of core polarization, and also because, as we have demonstrated, the bare G -matrix can be calculated quite accurately. Thus it appears that one can now derive the effective interaction for halo nuclei much more accurately than for ordinary nuclei. We enthusiastically believe that the halo nuclei, which have already greatly enhanced our knowledge about nuclei, may in addition provide a more accurate testing ground for the fundamental NN interaction, than the ordinary nuclei.

This work is supported in part by the USDOE Grant DE-FG02-88ER40388, by the NSF Grant and by the Fundación Antorchas (Argentina). One of us (T.T.S. Kuo) is grateful for the warm hospitality extended to him while visiting the Universidad Nacional de La Plata.

REFERENCES

- [1] S.M. Austin and G.F. Bertsch, *Scientific American* **272** 90 (1995).
- [2] W. Nazarewicz *et al.*, *Phys. Rev.* **C53** 740 (1996).
- [3] I. Hamamoto, H. Sagawa, and X.L. Zhang, *Phys. Rev.* **C53** 765 (1996); I. Hamamoto and H. Sagawa, *Phys. Rev.* **C53** 1492 (1996).
- [4] R.D. Page *et al.*, *Phys. Rev.* **C53** 660 (1996).
- [5] M.V. Zhukov *et al.*, *Phys. Rep.* **231**, 151 (1993), and refs. therein.
- [6] M. Lacombe *et al.*, *Phys. Rev.* **C21** 861 (1980).
- [7] R. Machleidt, *Adv. Nucl. Phys.* **19** (1989) 189.
- [8] T.T.S. Kuo and E. Osnes, *Lecture Notes in Physics* **Vol.364** (Springer-Verlag 1990) p. 1.
- [9] T.T.S. Kuo, E. Krmpotić, K. Suzuki and R. Okamoto, *Nucl. Phys.* **A582**, (1995) 205.
- [10] T.T.S. Kuo, H. Muether and Azimi-Nilli, to be published in *Festschrift commemorating G.E. Brown's 70th birthday* (North-Holland Elsevier 1996).
- [11] S.F. Tsai and T.T.S. Kuo, *Phys. Lett.* **B39** 427 (1972).
- [12] E.M. Krenciglowa, C.L. Kung, T.T.S. Kuo and E. Osnes, *Ann. Phys. (N.Y.)* **101**, 154 (1976).
- [13] H. Müther and P. Sauer, in *Computational Nuclear Physics* 2, ed. by K. Langanke, J.A. Maruhn and S. Koonin, Springer-Verlag 1992, p. 30.
- [14] J. Shurpin, T.T.S. Kuo, and D. Strottman, *Nucl. Phys.* **A408**, 310 (1983).
- [15] M. Hjorth-Jensen, T.T.S. Kuo and E. Osnes, *Phys. Rep.* **261** (1995) 126.
- [16] J.K. Tuli (editor), *Nuclear Wallet Cards*, National Nuclear Data Center, Brookhaven

National Laboratory (1995)

TABLES

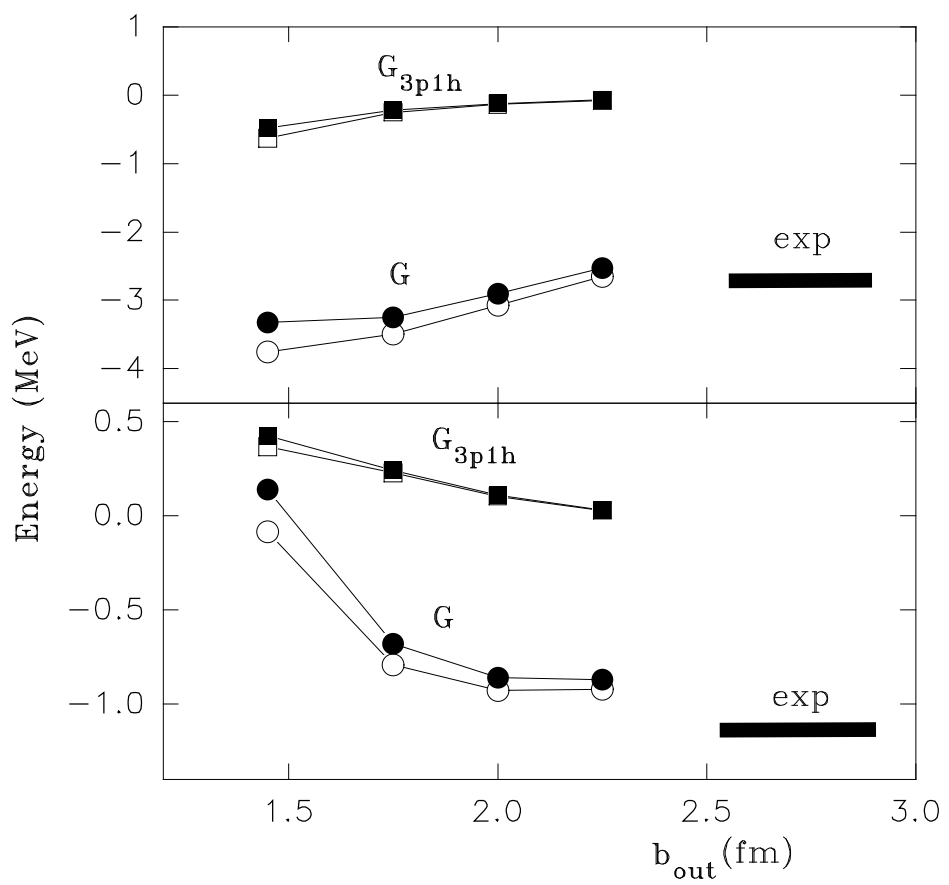
TABLE I. Dependence of the two-frequency G -matrix on the choice of n_3 . Listed are the matrix element $\langle (0p_{3/2})^2; TJ | G(\omega) | (0p_{3/2})^2; TJ \rangle$ (in MeV), calculated for the Paris potential and three different values of ω (in MeV), with $TJ = 01$ (upper panel) and with $TJ = 10$ (lower panel). We have used $b_{in} = 1.45$ and $b_{out} = 2.0$ fm for the length parameters, and $n_1 = 1$ and $n_2 = 6$ for the exclusion operator. The first row in each group (F) denotes the free G -matrix.

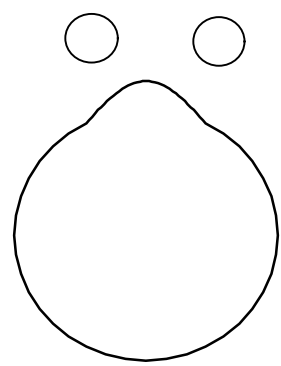
n_3	$\omega = -5$	$\omega = -10$	$\omega = -20$
F	−6.896	−4.530	−3.155
6	−2.218	−2.115	−1.885
15	−2.217	−2.114	−1.882
21	−2.217	−2.114	−1.882
F	−4.422	−3.933	−3.480
6	−2.768	−2.748	−2.701
15	−2.761	−2.744	−2.698
21	−2.761	−2.744	−2.698

Figure Captions

Fig. 1 Diagonal matrix elements of G_{3p1h} and G for the states $|(p_{3/2})^2; T = 1, J = 0\rangle$ (upper panel) and $|(p_{1/2})^2; T = 1, J = 0\rangle$ (lower panel) as a function of b_{out} ; calculations done with Paris and Bonn-A potentials are shown by open and solid symbols, respectively. The G -matrix curves are for $\omega = -5$ MeV and Pauli exclusion operator with $(n_1, n_2, n_3) = (1, 3, 21)$.

Fig. 2. Comparison of core polarization in ordinary and halo nuclei.





Halo Nucleus



Normal Nucleus